Desalination and Water Treatment
www.deswater.com

doi: 10.5004/dwt.2020.24715

177 (2020) 102–108
February

Lithium sorption from aqueous solution with cationic resins

S. Güneysu

Department of Environmental Engineering, Faculty of Engineering, İstanbul University – Cerrahpasa, Avcilar, 34320 İstanbul, Turkey, email: guneysu@istanbul.edu.tr

Received 13 September 2018; Accepted 26 July 2019

ABSTRACT

In this work, sorption study focused on the lithium removal from water by resins. Adsorption of lithium on activated carbon is limited, but the usage of ion exchange resin has yielded better correlations with the isotherms of Freundlich, Langmuir, Dubinin–Radushkevich and Temkin. In this work, sorption of lithium, from aqueous solutions was investigated; with strong acidic typical cationic Na^+ form (Armfield) and weak acidic cationic resin H^+ form (Lewatit CNP 80). Optimum sorption conditions were studied with pH and temperature effect, resin dose, lithium concentration and contact time. The optimum conditions for sorption of lithium were found as 0.1 g/L resin dose, 50 ppm lithium solution, at pH 6, 20°C temperature and 90 min contact time. Comparing the correlation coefficients, sorption of lithium with weak acidic resin fits better than the strong acidic resin. Langmuir model and pseudo-second-order kinetics describe that the adsorption of lithium by weak acidic cationic resin fits better.

Keywords: Sorption; Lithium; Cationic resin; Metal removal; Isotherm

1. Introduction

The environmental effects of metals that are found in nature are in different forms and highly variable. Over the decades, compounds that are used extensively expended in industrial applications have accumulated in the water and have unpredictable negative consequences. Lithium is in the class of alkali metals and is widely available in the earth's crust. Lithium and its compounds have been widely used in different applications, for example; lithium is the main material in production of lithium carbonate that is used to treat mania [1]. Lithium and its compounds have been extensively expended in ceramic, glassware, batteries, lubricant production, and alloy hardeners. Because of its relative transparency to neutron, Li has been used as a coolant in nuclear power plants. Water containing 1.7 mg/L lithium is called "Crazy Water" because of its relaxing and therapeutic effect. Lithium can be found in high concentrations in surface water resources and it is non-biodegradable. Although lithium has low environmental toxicity, it is not a nutritional mineral for plants and at elevated overdose it is toxic [2].

Due to the recent developments of electrical motive devices, lithium demand and consumption has incremented exponentially, thus the price of lithium [3]. The average concentration of lithium is about 0.006% in the earth's crust, while in seawater it is reported to be about 0.17 mg/L [4]. For this reason, extracting lithium from seawater can be a possible solution to supplement the ever-increasing demand of lithium. The separation of lithium from the aqueous solution provides both public health benefits and economic benefits. Different approaches have been applied in recovery of lithium from aqueous solution, and these include extraction [5], chemical precipitation [6], electrochemical [7], nanofiltration [8], accumulation with microorganisms [9], electrodialysis [10], ion exchange [11] and adsorption [4,12].

Of these, adsorption process is mostly preferred due to the regeneration of adsorbent, low sludge formation, low

operating costs, effective and easy process. Consequently, a number of lithium sorption studies with active carbon adsorption or adsorption with ion-exchange resin have been investigated. These include amberlite [13], nano-crystal MnO_2 [14], manganese (III) oxide nanopowder [4,15], strongly acidic, hydrogen form ion-exchange resin [16], aluminosilicate MCM 41 [17], activated carbon [17]. These studies have demonstrated removal and/or recovery efficiencies for the lithium ion of the adsorbent and ion exchangers in different types. However, it has been found that light metal ions such as amberlite, lithium ion (Li^+), and a strong acidic cation exchange with Na^+ and H^+ are suitable for aqueous solution recovery and that the exchange with Na^+ ion has a higher ion exchange capacity [13,17]. The capacity of the ion-exchange resin depends mainly on the functional group, cationic form and pore structure.

The use of cationic resin in recovery of lithium has not been fully explored. Therefore, in this study, the use of ion exchange resins in lithium adsorption; optimum conditions for pH, resin dosing and contact time were determined. The Freundlich, Langmuir, Dubinin–Radushkevich and Temkin equations were used to fit the equilibrium isotherms. Pseudo-first and pseudo-second order equations were used for describing the sorption process.

2. Materials and methods

The ion-exchange resins used in the study were selected according to their cationic and porosity properties. As commercial names, Lewatit® CNP 80 ion-exchange resin has properties of weak acidic, H^+ form, macro-porous, and acrylic-based cationic ion exchange resin whereas the other resin is called as Armfield; a typical commercially strong acidic cationic resin and Na^+ form. The properties of these ion-exchange resins are given in Table 1.

In experimental studies, synthetic lithium solutions was prepared with analytical pure Li_2CO_3 (Sigma-Aldrich Chemie GmbH, Sigald, 554-13-2) in distilled water. First, batch studies were carried out pH values 2, 4, 6, 8 and 10, resin doses 0.1, 0.2, 0.5, 1 and 5 g, temperatures 20°C, 30°C, 40°C and 50°C and 10, 25, 50, 75 and 100 ppm lithium concentrations. To adjust the pH of the solution, 0.1 M H_2SO_4 and 0.1 M NaOH were used. The effect of each condition is determined while holding the other variables constant. In experimental studies, 100 mL of 50 ppm Li(I) synthetic solution was put in 250 mL conical flask and 0.1–5.0 g various resin doses was added. Solutions were shaken in an incubator shaker at 160 rpm at predetermined optimum removal times. The temperature throughout the batch studies was first kept at 20°C. Sorption studies were first focused to research on optimum resin dose and sorption time, then the temperature and pH variation effects were studied. Sorption studies showed that the most effective removal capacity was at 20°C temperature and at pH 6. After this point, study was carried out at 20°C temperature and at pH 6. At the end of shaking, the samples were filtered and the concentration was resolute by Dionex ion chromatography ICS 1100 with Degas, Chromeleon SE. For determination of Li^+, Na^+, K^+ and Ca^{2+}, an analytical column CS16 and Guard column CG16 (both 3 × 50 mm) and CSRS-I (2 mm) suppressor in a chemical mode were expended.

10 mmol methanesulfonic acid was used as an eluent at flow rate of 1.0 mL/min. 25 μL injection volume was selected for all detections. Peak identification was confirmed based on a match of ion chromatograph retention times and standard samples. Limits of detection were determined as mean of three times standard deviation of the field blank value and the value corresponded to a range of 0.021 to 0.083 ng/L for cations. Limits of quantification were between 0.063 and 0.252 ng/L for cations. The ion exchange capacity at time t, q_t (mg/g), was calculated using the following formula:

$$q_t = \frac{\left(C_0 - C_t\right)V}{W} \tag{1}$$

where C_t (mg/L) is the lithium concentration of liquid phase at any time, C_0 (mg/L) is the initial lithium concentration of the lithium in solution. V is the volume of the solution (L) and W is the mass of ion exchanged resin (g). At equilibrium, q_e (mg/g) was calculated using the formula:

$$q_e = \frac{\left(C_0 - C_e\right)V}{W} \tag{2}$$

where C_0 and C_e (mg/L) are initial concentration and the concentration of lithium ion at equilibrium, respectively.

Table 1
Properties of ion exchange resins studied

Properties	Ion exchange resins	
	Weak acidic cationic resin (Lewatit CNP 80)	Strong acidic cationic resin (Armfield)
Appearance	Yellow white, opaque beads	Amber, clear spherical beads
Structure	Macro porous	Gel cross-linked
Functional group	–COO–	$–SO_3^-$
Ionic form	H^+	Na^+
Bulk density, g/L	750	780–880
Total capacity, eq/L	4.3	1.9–2.0
Bead size, mm	0.4–1.6	0.315–1.25
Stability at pH range	0–14	6–9

V is the volume of aqueous lithium solution and W (g) is the amount of ion exchange resin.

3. Results and discussion

3.1. pH effect

Fig. 1 shows the pH effect on resins sorption capacity. Initial values about lithium concentration, process temperature and resins amount were 50 ppm, 20°C and 0.1 g, respectively.

From Fig. 1, ion exchange capacity is very low at pH 4 and increases maximum capacity at pH 6. This is related to the competition of hydrogen and lithium ions during the sorption of resins at around neutral pH values. However, over pH 6, the ion exchange capacity decreases because of the precipitation of lithium.

3.2. Temperature effect

Fig. 2 shows the variation of temperature effect on resin's sorption capacity. Removal capacity of lithium is higher at low temperatures nearly 20°C. Along with the increasing temperatures, removal capacity decreases by decomposition of resin.

3.3. Lithium ion concentration effect

In Figs. 3 and 4, the effect of lithium concentration can be observed over time on the sorption capacity with Lewatit CNP 80 and Armfield resins. As the concentration of lithium is increased, the equilibrium capacity also increases. The adsorption rate is higher in the first 20 min, after that which the rate increases steadily. This attributed to the fact that, at the beginning, they are readily available sites for sorption.

3.4. Equilibrium studies

The equilibrium curves of the lithium cation sorption with Lewatit CNP80 and Armfield resins are shown in Figs. 5 and 6, respectively. In the Lewatit CNP80 sorption, the isotherm increases with the increase of C_e and q_e at the beginning and it becomes linear afterwards. This suggests that the ion-exchange resin has an increased capacity for lithium ions. For a typical cationic resin, curve of isotherms by the experimental data reveals a poor capacity. This indicates that Armfield resin does not have a suitable sorption capacity for lithium ions. The adsorption isotherms of lithium are investigated using Langmuir, Freundlich, Temkin and Dubinin–Radushkevich.

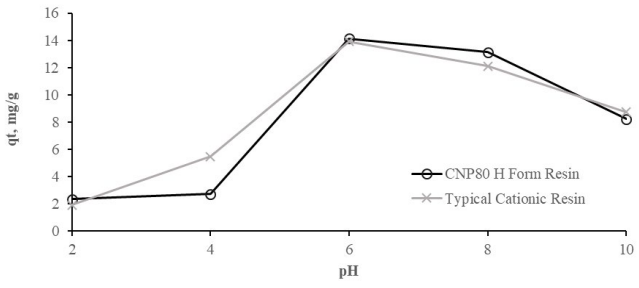

Fig. 1. Effect of pH on resins sorption capacity.

3.4.1. Freundlich isotherm

In heterogeneous systems, usually Freundlich isotherm is applied [18–21]. The Freundlich equation can be written as:

$$q_e = K_F C_e^{\frac{1}{n}} \tag{3}$$

If we linearize the equation:

$$\log q_e = \log K_F + \frac{1}{n}\log C_e \tag{4}$$

K_F and n can be defined as Freundlich isotherm constants and exponent, respectively. K_F and n can be calculated

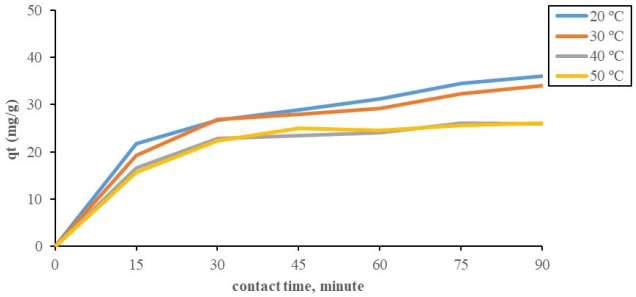

Fig. 2. Effect of temperature on sorption capacity of CNP80 H^+ form resin.

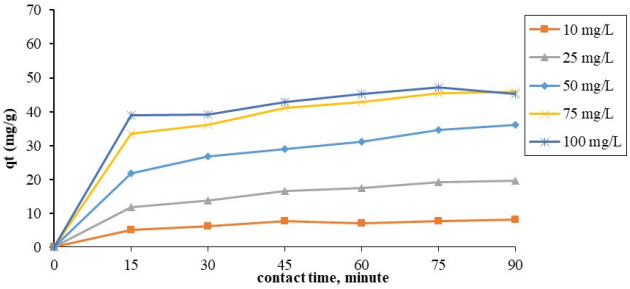

Fig. 3. Effect of resin (Lewatit CNP 80) capacity with initial lithium concentration.

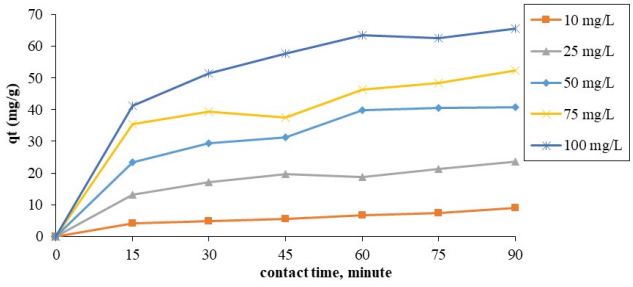

Fig. 4. Effect of resin (Armfield) capacity with initial lithium concentration.

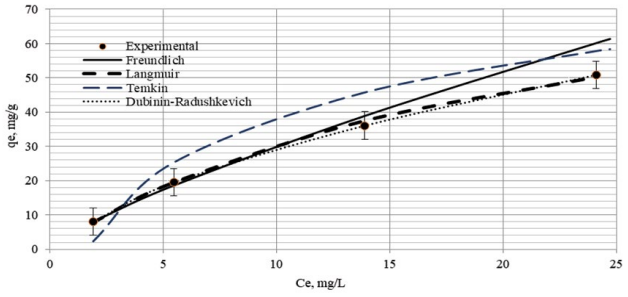

Fig. 5. Isotherms of lithium sorption on Lewatit CNP80 resin.

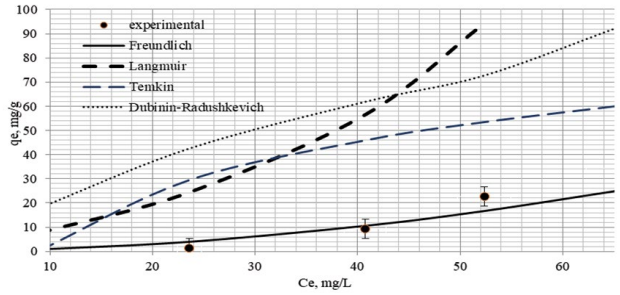

Fig. 6. Isotherms of lithium sorption on Armfield resin.

from the log of q_e and C_e. Freundlich isotherm constants and correlation coefficients are given in Tables 2 and 3.

3.4.2. Langmuir isotherm

Langmuir isotherm can be expressed as below and has much of applications on sorption processes [22,23]:

$$q_e = \frac{K_L C_e}{1 + a_L C_e} \tag{5}$$

This expression can be linearized as:

$$\frac{C_e}{q_e} = \frac{1}{K_L} + \frac{a_L}{K_L} C_e \tag{6}$$

q_e (mmol/g) is the amount of adsorbed lithium per unit weight of adsorbent and C_e (mmol/L) is the unadsorbed lithium concentration in solution at equilibrium. K_L is the Langmuir equilibrium constant where the K_L/a_L defines the theoretical monolayer saturation capacity, Q_0. Therefore, a_L/K_L and $1/K_L$ can be found from graphic of C_e/q_e to C_e, line of slope and interception, respectively.

The Langmuir constants a_L, K_L, Q_0 and the correlation coefficients are listed in Tables 2 and 3 for the lithium-Lewatit CNP80 and Armfield system. Figs. 5 and 6 show the Langmuir isotherm and its experimental data. The monolayer saturation capacity, Q_0, is 93.45 mg/g. In all cases, the Langmuir isotherm correlation coefficients fit better than the other isotherms applied in this study (Fig. 5).

3.4.3. Dubinin–Radushkevich isotherm

Very similar to Langmuir isotherm, The Dubinin–Radushkevich isotherm have also applied for metal ion and acid dye sorption on surfactant and activated carbon, respectively [24,25]. The Dubinin–Radushkevich equation can be described as:

$$q_e = q_m e^{-\beta\varepsilon^2} \tag{7}$$

A linear form of equation is:

$$\ln q_e = \ln q_m - \beta\varepsilon^2 \tag{8}$$

q_m: is the monolayer capacity of Dubinin–Radushkevich (mmol/g), β: a constant related to sorption energy and ε: the Polanyi potential and can be described as below:

$$\varepsilon = RT \ln\left(1 + \frac{1}{C_e}\right) \tag{9}$$

where R is the gas constant (8.314 J/mol K) and T is the absolute temperature. The constant β gives the mean free energy. E can be calculated from the equation below and means by transferring to the solid surface from solution, defined as sorption of the sorbate molecule when it is transferred to the surface of the solid from infinity in the solution and can be computed [24,25].

$$E = \frac{1}{\sqrt{2\beta}} \tag{10}$$

Tables 2 and 3 give the Dubinin–Radushkevich constants that are calculated from the data of plot in Figs. 5 and 6, respectively. In addition, the correlation coefficient has been determined in Tables 2 and 3. The data of isotherm are the lowest of all applied isotherms. Hence, the Langmuir equation fits better than the other applied isotherms of Freundlich, Temkin and Dubinin–Radushkevich equations (Fig. 5). Analysis of mean free energy shows that adsorption was favoured since $E < 8$ kJ/mol [12].

Table 2
Langmuir, Freundlich, Temkin and Dubinin–Radushkevich isotherms constants for Lewatit CNP 80 sorption

Langmuir			Freundlich			Temkin			Dubinin–Radushkevich			
Q_0 (mg/g)	b (L/mg)	R^2	K_F (L/g)	n	R^2	B (mg/g)	A (L/mg)	R^2	q_m (mg/g)	β	E kJ/mol	R^2
93.45	0.05	0.992	4.88	1.27	0.975	21.91	1.72	0.823	45.46	1.73	0.54	0.792

Table 3
Langmuir, Freundlich, Temkin and Dubinin–Radushkevich isotherms constants for Armfield sorption

Langmuir			Freundlich			Temkin			Dubinin–Radushkevich			
Q_0 (mg/g)	b (L/mg)	R^2	K_F (L/g)	n	R^2	B (mg/g)	A (L/mg)	R^2	q_m (mg/g)	β	E kJ/mol	R^2
–69.93	–0.02	0.82	0.011	0.544	0.85	30.15	8.85	0.825	46.55	27.40	0.135	0.782

3.4.4. Temkin isotherm

The Temkin isotherm can be calculated from the equation below [24]:

$$q_e = \frac{RT}{b}\ln\left(AC_e\right) \tag{11}$$

Linearized form of the equation is as below:

$$q_e = \frac{RT}{b}\ln A + \frac{RT}{b}\ln C_e \tag{12}$$

where

$$\frac{RT}{b} = B \tag{13}$$

By Eq. (12), the sorption data analysed easily. Hence, A and B constants can be calculated from a plot of q_e to ln C_e. Temkin isotherm constants are given in Tables 2 and 3, and Fig. 5. The Temkin correlation coefficient is given in Table 2, where the values are in the middle of Dubinin–Radushkevich and Freundlich values. Therefore, the Temkin isotherm fits better than the Dubinin–Radushkevich and Freundlich (Fig. 6).

3.5. Kinetic studies

In Fig. 2 sorption of lithium increases by the time until at the end of equilibrium time of 90 min. The initial lithium concentration and temperature never changes the equilibrium time in this study. For the purpose of examining the mass transfer and chemical reactions of adsorption process, a kinetic model has to be analysed. Transportation of absorbates into the adsorbents in batch reactors have been widely applied and defines for the models of homogeneous surface diffusion model, pore diffusion model, and heterogeneous diffusion model [26,27]. The large number and array of different functional groups on the Lewatit CNP80 ion-exchange resin imply that there are different types of adsorbent–adsorbate interactions, thus a need to identify a suitable kinetic isotherm.

3.5.1. Pseudo-first-order model

Pseudo-first-order equation gives the sorption kinetics [26,28,29]. The differential equation is the following:

$$\frac{dq_t}{dt} = k_1\left(q_e - q_t\right) \tag{14}$$

By editing Eq. (14) with the initial conditions q_t = 0 at t = 0 and $q_t = q_t$ at $t = t$, it becomes:

$$\log\left(\frac{q_e}{q_e - q_t}\right) = \frac{k_1}{2{,}303}t \tag{15}$$

Eq. (15) can be linearized as:

$$\log\left(q_e - q_t\right) = \log q_e - \frac{k_1}{2.303}t \tag{16}$$

where q_e is the amount of lithium adsorbed and q_t is the amount at equilibrium time (mmol/g). The equilibrium rate constant of pseudo-first-order adsorption is defined as k_1 (1/min).

A plot of linearized form of kinetic model about adsorption can be shown in Fig. 7. The first-order rate constant, k_1, and equilibrium adsorption density, q_e, were calculated from the slopes and intercepts of plots of log (q_e–q_t) vs. time. In addition to this, the experimental data diverged from the data calculated by equations. Correlation coefficients of the results are listed in Table 4. The correlation coefficients for the kinetic model at studied concentrations show nominal values. According to kinetic model values calculated, q_e was out of standard range of value. This means that sorption system is not fitted to the first order model.

3.5.2. Pseudo-second-order model

The adsorption kinetics may also be calculated by a pseudo-second-order equation [26,29,30]. The differential equation is given below:

$$\frac{dq_t}{dt} = k_2\left(q_e - q_t\right)^2 \tag{17}$$

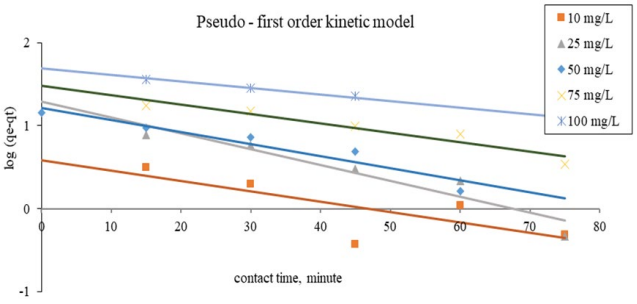

Fig. 7. Linear pseudo-first-order model for the sorption kinetics of lithium onto Lewatit CNP80.

Table 4
Kinetics for lithium sorption onto Lewatit CNP80 resin

C_0, mg/L	q_e, mg/g	Pseudo-first-order		Pseudo-second-order	
		k_1	R^2	k_2	R^2
10	8.085	0.02878	0.5726	0.00857	0.9853
25	19.524	0.04398	0.9021	0.00246	0.9931
50	36.094	0.03339	0.9125	0.00141	0.9898
75	50.885	0.02602	0.9161	0.00111	0.9820
100	75.265	0.01819	0.9951	0.00042	0.9163

Integration of Eq. (17) by the boundary conditions gives:

$$\frac{1}{\left(q_e - q_t\right)} = \frac{1}{q_e} + k_2 t \tag{18}$$

Eq. (18) can be linearized as:

$$\frac{1}{q_t} = \frac{1}{k_2 q_e^2} + \frac{1}{q_e} t \tag{19}$$

where k_2 is determined as the equilibrium rate constant of kinetic model (g/mmol min).

k_2 and q_e that are the constants of model were calculated from the slopes and intercepts of plots t/q_t vs. time. Fig. 8 shows a plot of t/q_t vs. t, which shows a good agreement of experimental data with the second-order kinetic model for different initial lithium concentrations. Table 4 gives the results obtained from the second-order kinetic model plot. The correlation coefficients (R^2) for the second-order kinetic model calculated were greater than 0.9163 for all adsorptions studied. The q_e values obtained, also fit very well with the experimental data. These indicate that the lithium sorption studied, shows a good adaptation to pseudo-second-order kinetic model.

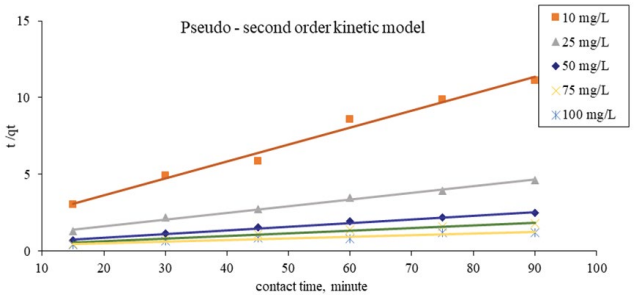

Fig. 8. Linear pseudo-second-order model for the sorption kinetics of lithium onto Lewatit CNP80.

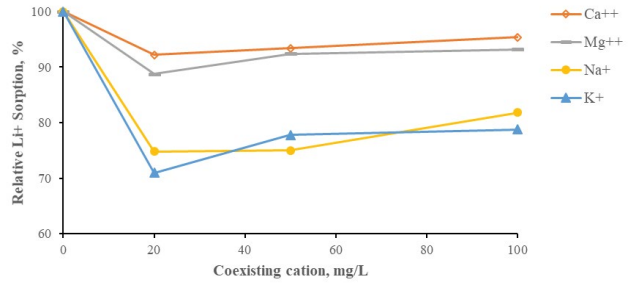

Fig. 9. Competition of sorption with Na^+, K^+, Ca^{++} and Mg^{++} ions.

3.6. Competition of sorption in other ions presence

Fig. 9 shows that sorption in competition with K^+, Na^+, Mg^{++} and Ca^{++} ions 0–20–50 and 100 mg/L of solutions mixed with 50 ppm lithium solution.

3.7. Regeneration of resin

Regeneration is the key of applicability of the adsorption system. In this study, after calculating the optimized conditions of adsorption, regeneration of resin was investigated. Regeneration of resin is usually made with HCl or NaClO chemicals [31]. In this study, because of being a very common agent and having efficient advantages, HCl was used for regeneration. Fig. 10 shows that during regeneration cycles, adsorption capacity of resin was decreased due to cycles. Regeneration of resin was carried out in five cycles after each adsorption study. 1 M HCl was used for regeneration and after five cycles of regeneration, structure of resin was increasingly decomposed and this decreases the adsorption capacity. This can be explained by the use of highly oxidative chemical HCl, which might have a damage on resin surface [32].

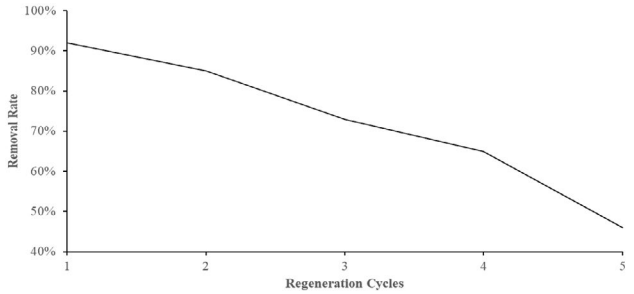

Fig. 10. Effect of regeneration cycle with HCl.

4. Conclusion

In the present study, sorption capacity of two different types of commercial resins has been investigated. Weak acidic cationic resin as commercial name Lewatit CNP80 resin favoured the lithium sorption against the strong acidic resin known as Armfield.

Temperature effect on the sorption in this study was also studied. Temperatures between 20°C and 50°C are studied, lower removal capacities at higher temperatures are observed because of a decomposition of resin. The highest removal capacity was calculated at 20°C temperature at which the study was carried out.

The isotherms of Langmuir, Freundlich, Temkin and Dubinin–Radushkevich were applied and the sorption of resins and constants was given in Tables 2 and 3. It is clear that Langmuir model describes the Lewatit CNP80 sorption system better than Armfield system.

Pseudo-first and second-order kinetics calculated only for Lewatit CNP80 system and kinetics proved the best correlation of the experimental data studied.

Overall, for practical desorption and recycling studies were run, with 1 M HCl and for five cycles, structure of resin was increasingly decomposed and this decreases the adsorption capacity.

Funding

This research did not receive any specific grant from funding agencies in the public, commercial, or non-for-profit sectors.

References

[1] M.P. Freeman, S.A. Freeman, Lithium: clinical considerations in internal medicine, Am. J. Med., 119 (2006) 478–481.
[2] H. Aral, A. Vecchio-Sadus, Toxicity of lithium to humans and the environment—a literature review, Ecotoxicol. Environ. Saf., 70 (2008) 349–356.
[3] L.T. Peiró, G.V. Méndez, R.U. Ayres, Lithium: sources, production, uses, and recovery outlook, JOM, 65 (2013) 986–996.
[4] K.S. Chung, J.C. Lee, E.J. Kim, K.C. Lee, Y.S. Kim, K. Ooi, Recovery of lithium from seawater using nano-manganese oxide adsorbents prepared by gel process, Mater. Sci. Forum, 449 (2004) 277–280.
[5] T. Takeuchi, Extraction of lithium from sea water with metallic aluminium, J. Nucl. Sci. Technol., 17 (1980) 922–928.
[6] K. Yanagase, T. Yoshinaga, K. Kawano, T. Matsuoka, The recovery of lithium from geothermal water in the Hatchobaru Area of Kyushu, Japan, Bull. Chem. Soc. Jpn., 56 (1983) 2490–2498.
[7] H. Kanoh, K. Ooi, Y. Miyai, S. Katoh, Electrochemical recovery of lithium ions in the aqueous phase, Sep. Sci. Technol., 28 (1993) 643–651.
[8] X. Wen, P. Ma, C. Zhu, Q. He, X. Deng, Preliminary study on recovering lithium chloride from lithium-containing waters by nanofiltration, Sep. Purif. Technol., 49 (2006) 230–236.
[9] T. Tsuruta, Removal and recovery of lithium using various microorganisms, J. Biosci. Bioeng., 100 (2005) 562–566.
[10] T. Hoshino, Preliminary studies of lithium recovery technology from seawater by electrodialysis using inic liquid membrane, Desalination, 317 (2013) 11–16.
[11] S. Zandevakili, M. Ranjbar, M. Ehteshamzadeh, Recovery of lithium from Urmia Lake by a nanostructure MnO_2 ion sieve, Hydrometallurgy, 149 (2014) 148–152.
[12] G. Xiao, K. Tong, L. Zhou, J. Xiao, S. Sun, P. Li, J. Yu, Adsorption and desorption behaviour of lithium ion in spherical PVC–MnO_2 ion sieve, Ind. Eng. Chem. Res., 51 (2012) 10921–10929.
[13] A. Navarrete-Guijosa, R. Navarrete-Casas, C. Valenzuela-Calahorro, J.D. Lopez-Gonzalez, A. García-Rodríguez, Lithium adsorption by acid and sodium amberlite, J. Colloid Interface Sci., 264 (2003) 60–66.
[14] Q.H. Zhang, S. Sun, S. Li, H. Jiang, J.G. Yu, Adsorption of lithium ions on novel nanocrystal MnO_2, Chem. Eng. Sci., 62 (2007) 4869–4874.
[15] K. Ooi, Y. Miyai, S. Katoh, Recovery of lithium from seawater by manganese oxide adsorbent, Sep. Sci. Technol., 21 (1986) 755–766.
[16] W. Yi, C. Yan, P. Ma, Removal of calcium and magnesium from $LiHCO_3$ solutions for preparation of high-purity Li_2CO_3 by ion-exchange resin, Desalination, 249 (2009) 729–735.
[17] J. Lemaire, L. Svecova, F. Lagallarde, R. Laucournet, P.X. Thivel, Lithium recovery from aqueous solution by sorption/desorption, Hydrometallurgy, 143 (2014) 1–11.
[18] N.M. Agyei, C.A. Strydom, J.H. Potgieter, An investigation of phosphate ion adsorption from aqueous solution by fly ash and slag, Cem. Concr. Res., 30 (2000) 823–826.
[19] K. Sakadevan, H.J. Bavor, Phosphate adsorption characteristics of soils, slags and zeolite to be used as substrates in constructed wetland systems, Water Res., 32 (1998) 393–399.
[20] S. Baup, C. Jaffre, D. Wolbert, A. Laplanche, Adsorption of pesticides onto granular activated carbon: determination of surface diffusivities using simple batch experiments, Adsorption, 6 (2000) 219–228.
[21] D.S. Bhargava, S.B. Sheldarkar, Use of TNSAC in phosphate adsorption studies and relationships – literature, experimental methodology, justification and effects of process variables, Water Res., 27 (1993) 303–312.
[22] A.K. Bajpai, M. Rajpoot, D.D. Mishra, Static and kinetic studies on the adsorption behaviour of sulfadiazine, Adsorption, 6 (2000) 349–357.
[23] A.N. Onar, N. Balkaya, T. Akyuz, Phosphate removal by adsorption, Environ. Technol., 17 (1996) 207–213.
[24] K.K.H. Choy, G. McKay, J.F. Porter, Sorption of acid dyes from effluents using activated carbon, Resour. – Conserv. Recyl., 27 (1999) 57–71.
[25] S.H. Lin, R.S. Juang, Heavy metal removal from water by sorption using surfactant-modified montmorillonite, J. Hazard. Mater., 92 (2002) 315–326.
[26] W.J. Wu, R.K. Tang, M. Haas, G.H. Nancollas, Constant composition dissolution of mixed phases, J. Colloid Interface Sci., 244 (2001) 347–352.
[27] V. Doğan, S. Aydın, Vanadium (V) removal by adsorption onto activated carbon derived from starch industry waste sludge, Sep. Sci. Technol., 49 (2014) 1407–1415.
[28] G. Annadurai, R.S. Juang, D.J. Lee, Use of cellulose-based wastes for adsorption of dyes from aqueous solutions, J. Hazard. Mater., 92 (2002) 263–274.
[29] Y.S. Ho, C.C. Chiang, Sorption studies of acid dye by mixed sorbents, Adsorption, 7 (2001) 139–147.
[30] Y.S. Ho, G. McKay, Pseudo-second order model for sorption processes, Process Biochem., 34 (1999) 451–465.
[31] H. Selçuk, A. Öngen, B. Yüzer, M.İ. Aydin, H.E. Ökten, Comparison of ozonation and coagulation decolourization methods in real textile wastewater, Desal. Wat. Treat., 103 (2018) 55–64.
[32] M. Wawrzkiewicz, Removal of CI Basic Blue 3 dye by sorption onto cation exchange resin, functionalized and non-functionalized polymeric sorbents from aqueous solutions and wastewaters, Chem. Eng. J., 217 (2013) 414–425.